Rapid degradation pathways of host proteins during HCMV infection revealed by quantitative proteomics

Michael Weekes[1]

[1]University of Cambridge

June 30, 2020

Introduction

Human cytomegalovirus (HCMV) is a ubiquitous betaherpesvirus that persistently infects the majority of the human population worldwide (Cannon et al., 2010). Following primary infection under the control of a healthy immune system, a latent infection is established that persists lifelong (Reeves et al., 2005). Although primary infection is mostly asymptomatic in healthy individuals, HCMV may lead to significant morbidity or mortality in immunocompromised patients, particularly transplant recipients and AIDS patients (Griffiths et al., 2015). Vertical transmission of HCMV is a leading cause of congenital infection, resulting in deafness and intellectual disability in newborns (Manicklal et al., 2013). Existing therapies that either target the viral polymerase or terminase are associated with significant toxicity and/or sporadic resistance (El Helou and Razonable, 2019). The identification and characterisation of critical facets of host innate immunity that are targeted for degradation by HCMV proteins thus has important implications for antiviral therapy, since such interactions may be inhibitable by small-molecules, facilitating endogenous inhibition of viral replication (Nathans et al., 2008).

HCMV has been reported to disrupt interferon (IFN) production, neutralise the IFN response (Le-Trilling and Trilling, 2015;Goodwin et al., 2018), inhibit natural killer (NK) cell activation (Patel et al., 2018), and avoid T cell surveillance via downregulation of MHC molecules (Jackson et al., 2011). A common final pathway for many host protein targets is proteasomal or lysosomal degradation (Halenius et al., 2015). For example, HCMV facilitates viral replication by degrading components of cellular promyelocytic leukemia nuclear bodies (PML-NB) Sp100, MORC3 and DAXX that act as restriction factors (Kim et al., 2011;Tavalai et al., 2011;Schreiner and Wodrich, 2013;Sloan et al., 2016).

We previously developed three orthogonal proteomic/transcriptomic screens to quantify protein degradation early during HCMV infection, identifying 133 degraded proteins that were enriched in antiviral restriction factors. The power of this approach was demonstrated by our identification of helicase-like transcription factor (HLTF) as a novel restriction factor that potently inhibited early viral gene expression and was targeted by the HCMV protein UL145 (Nightingale et al., 2018). However, a global approach to identify the mechanism of HCMV-induced protein degradation is lacking. Our previous study employed the broad, non-selective inhibitor MG132, which is known to affect lysosomal cathepsins in addition to the proteasome (Wiertz et al., 1996), and leupeptin which is a naturally occurring protease inhibitor that can inhibit some proteasomal proteases in addition to the lysosome (Nightingale et al., 2018).

In this study, we used the selective proteasome inhibitor bortezomib (Chen et al., 2011) to identify proteins specifically targeted for proteasomal degradation during HCMV infection. This identified that the majority of proteins rescued from degradation by MG132 were also rescued by bortezomib, highlighting the role of viral subversion of the proteasome in immune evasion. Our data additionally provide a shortlist of proteins degraded by the proteasome early during infection that are enriched in known antiviral factors for further investigation.

1

Material and methods

Cells and cell culture

Primary human fetal foreskin fibroblast cells (HFFFs) immortalised with human telomerase (HFFF-TERTs) were maintained in Dulbecco's modified Eagle's medium (DMEM) supplemented with 10% v/v foetal bovine serum (FBS), 100 U/ml penicillin, and 100 μg/ml streptomycin at 37 °C with 5% CO_2 (DMEM/FBS/PS). HFFF-TERTs have been tested at regular intervals since isolation to confirm that human leukocyte antigen (HLA) and MHC Class I Polypeptide-Related Sequence A (MICA) genotypes, cell morphology and antibiotic resistance are unchanged.

Virus and virus titration

The recombinant HCMV (RCMV1111) used was derived by transfection of a BAC clone of HCMV strain Merlin, the genome of which is designated the reference HCMV sequence by the National Center for Biotechnology Information and was sequenced after 3 passages in vitro (Dolan et al., 2004;Stanton et al., 2010). Virus stocks were prepared from HFFF-TERTs as described previously (Nobre et al., 2019). Tissue culture supernatants were kept when a 100% cytopathic effect was observed, and were centrifuged to remove cell debris. Cell-free virus was pelleted from supernatant by centrifugation at $15,000 \times g$ for 2 h and then resuspended in fresh DMEM. Residual debris was removed from the resulting virus stocks by centrifugation at 10,000 x g for 1 min. Virus titration was achieved by intracellularly staining HCMV IE1/2 in HFFF-TERTs that had been infected with serially diluted HCMV. Cells were harvested 24 h post-infection, fixed in 4% paraformaldehyde, permeabilised with ice-cold methanol, blocked with human TruStain FcX Fc receptor blocking solution (Biolegend) and then subjected to primary (anti-HCMV IE1/2, mouse monoclonal 6F8.2, Millipore) and secondary (anti-mouse IgG conjugated with Alexa Fluor 488, Thermo) antibody incubation. Data was acquired by FACSCalibur (BD biosciences) and analysed with FlowJo software (BD biosciences). The percentage of infected cells was determined by the percentage of IE1/2 positive cells, which was used to calculate the titre of virus stock.

Virus infections and inhibitors

1×10^6 HFFF-TERTs were plated in a 25 cm^2 flask. After 24 h, the medium was changed to DMEM lacking FBS but with 4 μg/ml dexamethasone, as this approach has been shown to improve infection efficiency (Tanaka et al., 1984). After 24 h, the medium was changed to DMEM containing the requisite volume of HCMV strain Merlin stock to achieve MOI 5. Cells were gently rocked (5 rpm) for 2 h, and then the medium was changed to DMEM/FBS/PS. MG132 (Sigma) at 10 μM or bortezomib (Sigma) at a range of concentrations was added to the cell culture 12 h prior to sample collection. For 12 hpi experiments, inhibitors were added to the initial viral mixture used for infection, which was replaced with drug-containing fresh DMEM after the 2 h of incubation.

Quantitative tandem-mass-tag based proteomics analysis and statistical analysis

Methods of proteomics analysis were described in our previous publication (Nightingale et al., 2018), and are briefly described here with a detailed description in the supplementary information. Whole cell lysates were digested into peptides with LysC and trypsin, and equal amounts of peptide labelled with tandem-mass-tag (TMT) reagents. Enriched, labelled peptides were subjected to liquid chromatography coupled with multi-stage mass spectrometry (LC-MS3) prior to quantification of ~2,500 proteins in a single mass spectrometry analysis using an Orbitrap Fusion Lumos (Thermo). To acquire more comprehensive data, TMT-labelled peptide samples were subjected to high pH reversed-phase fractionation (HpRP) to generate 12 combined peptide fractions prior to mass spectrometry. Mass spectra were processed using a SEQUEST-based software pipeline for quantitative proteomics, "MassPike," through a collaborative arrangement with Professor Steven Gygi's laboratory at Harvard Medical School. The method of significance A was used to estimate the p-value that each ratio was significantly different to 1 using Perseus version 1.5.1.6 (Cox and Mann, 2008). Values were adjusted for multiple hypothesis testing using the method of Benjamini-Hochberg (Cox and Mann, 2008).

2

Results

Optimisation of bortezomib concentration for experiments in HFFF-TERTs

Bortezomib has been employed in a number of studies of human cell lines as a specific inhibitor of the proteasome. However, a wide range of concentrations have been used, from 0.1 to 20 μM (Price et al., 2011;Chui et al., 2019). To optimise conditions for proteomic analysis in HCMV-infected immortalized primary human foetal foreskin fibroblasts (HFFF-TERTs), a range of bortezomib concentrations were compared with 10 μM MG132, a concentration we previously showed to provide efficacious inhibition of protein degradation (**Figures 1, S1**) (Nightingale et al., 2018). TMT peptide labels and MS3 mass spectrometry enabled very precise protein quantitation, as well as multiplexed analysis of up to 11 samples in the same experiment.

For each protein, ratios of (HCMV with bortezomib) / HCMV and (HCMV with MG132) / HCMV were compared to quantify the relative efficacy of protein rescue. The trend of linear correlation and slope of the trend line both increased with increasing bortezomib concentration, with a gradient near to one for 2 μM bortezomib. At this concentration, the degree of rescue was most similar between MG132 and bortezomib, and 2 μM bortezomib at 12 h post infection (hpi) was therefore selected for detailed comparative analysis (**Figure 1A-B**)
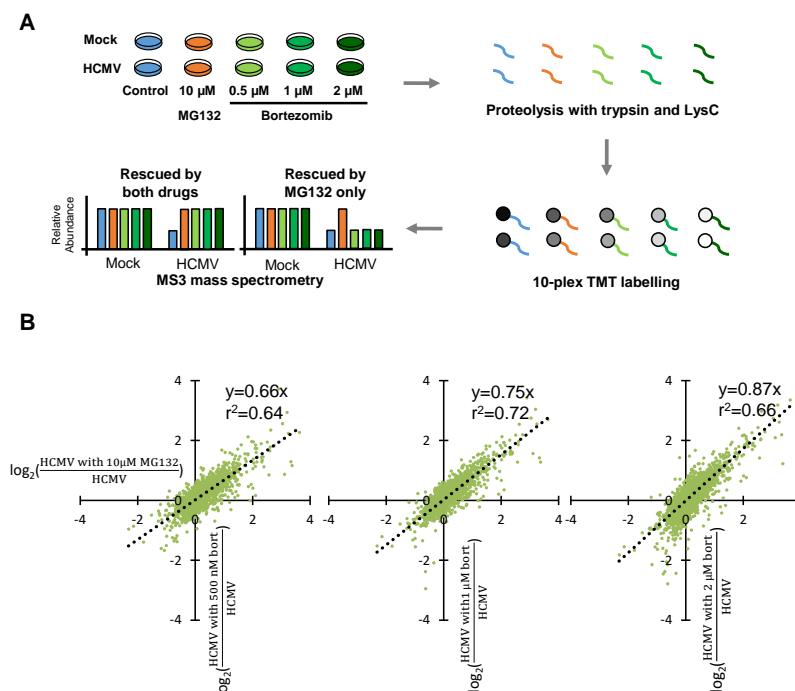
Figure 1

A

B

Φιγυρε 1. Οπτιμισατιον οφ βορτεζομιβ ςονςεντρατιον βψ ςομπαρισον ωιτη 10 μM ΜΓ132. (A) Schematic of the experimental workflow. HFFF-TERT cells were infected with Merlin strain HCMV (MOI 5) or mock infected and simultaneously treated with 10 μM MG132, 500 nM, 1 μM or 2 μM bortezomib. Samples were harvested at 12 hpi to maximise the ability to study very early infection as we previously described (Nightingale et al., 2018). Whole cell lysates were digested into peptides, which were labelled with TMT reagents followed by MS3 mass spectrometry. (B) Comparison of 10μM MG132 with 500 nM, 1 μM or 2 μM bortezomib (bort).

Multiple host proteins are targeted for proteasomal degradation early during HCMV infection

To build a comprehensive mechanistic picture of host protein degradation early during HCMV infection, data from experimental samples described in**Figure 1A** (that included the 2 μM bortezomib condition) was analysed in detail. Overall, 7192 host proteins were quantified, 145 of which were down-regulated by

4

HCMV >1.5-fold (with p<0.01) compared to mock infection. MG132 and bortezomib 'rescue ratios' were calculated for each protein, obtained by comparing protein abundance during HCMV infection +/- inhibitor with protein abundance during mock infection +/- inhibitor (**Figure 2A**).

For simplicity and consistency with our previous study (Nightingale et al., 2018), a rescue ratio of >1.5-fold with p<0.01 was set as a threshold to identify proteins rescued by either MG132, bortezomib or both (**Figures 2A, Table S1**). Using these criteria, 64/145 (44%) proteins were considered to be rescued by either inhibitor, with 34/64 proteins rescued by both drugs. Notably, this group contained the known HCMV restriction factors Sp100, MORC3, DAXX and HLTF in addition to cell cycle regulating protein ANAPC1, all of which have been reported to be degraded by ourselves and others (**Figure 2B)** (Tran et al., 2010;Chen et al., 2011;Kim et al., 2011;Tavalai et al., 2011;Schreiner and Wodrich, 2013;Sloan et al., 2016;Nightingale et al., 2018).

Data from all proteomic experiments in this study are shown in**Table S2** . Here, the worksheet "Plotter" is interactive, enabling generation of graphs of protein expression of any of the proteins quantified.
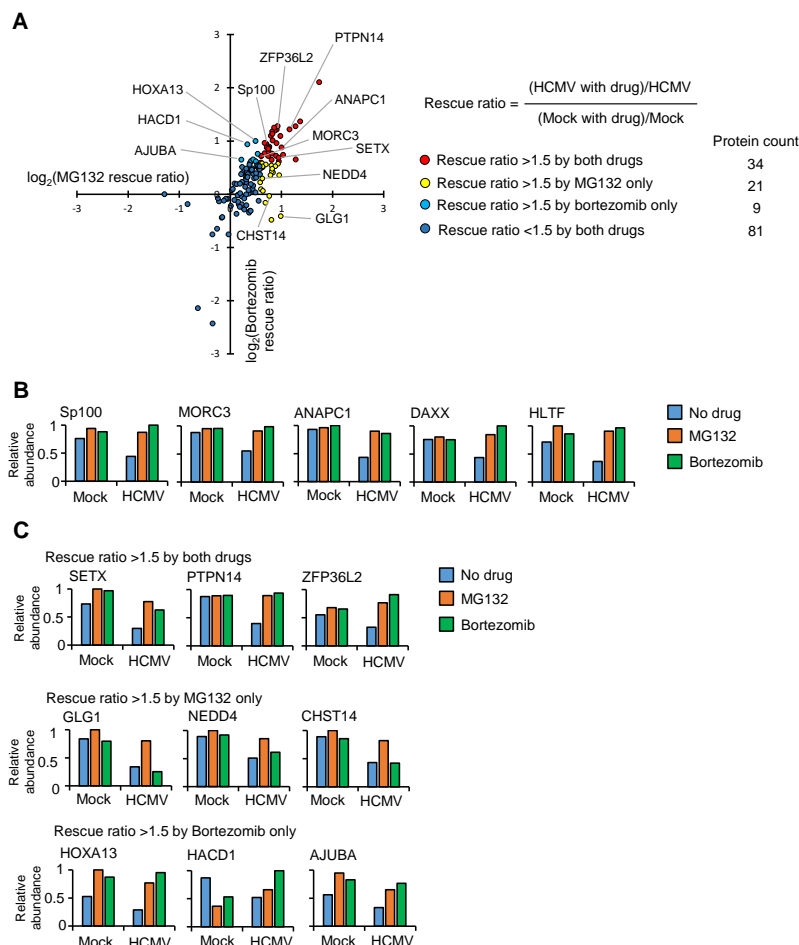
5

Figure 2

Figure 2. Identification of proteins targeted for degradation by HCMV using an inhibitor-based proteomic screen. (A) Results of the inhibitor-based screen. All 145 proteins downregulated >1.5 fold are plotted, with down-regulated proteins divided into 4 groups using rescue ratios of >1.5 as cut-offs. The table shows the number of proteins in each group. For rescue ratios, the denominator (mock with drug)/mock was limited to a minimum of 1 to prevent artificial ratio inflation. (B) Examples of positive controls from the existing literature that were validated in this screen. (C) Examples of degraded proteins rescued by both inhibitors (top panels), MG132 only (middle panels), or bortezomib only (bottom panels).

Certain proteins exhibited a greater degree of rescue with MG132 compared to bortezomib (**Figure 2B, yellow dots**). Of the 21 proteins only rescued >1.5 fold by MG132, 13 (62%) exhibited bortezomib rescue ratios of >1.25 and <1.5, suggesting that many of this group of proteins may nevertheless be proteasomally degraded. These included the PDZ domain containing protein 11 (PDZD11) and transcriptional repressor BEN Domain Containing 3 (BEND3) (**Figure S2, Tables S1-2**). In contrast, 8/21 proteins appeared gen-

uinely to be selectively rescued by MG132 but not bortezomib (bortezomib rescue ratio <1.25), including the fibroblast growth factor receptor Golgi Glycoprotein 1 (GLG1), E3 ligase Neural Precursor Cell Expressed, Developmentally Down-Regulated 4 (NEDD4) and carbohydrate sulfotransferase 14 (CHST14) (**Figure 2C middle panel, Table S1**). Similar data were obtained for treatments with 500 nM and 1 µM bortezomib, validating these findings (**Figure 3**). Interestingly, Gene Ontology annotation of all 8 proteins indicated an association with either the cell membrane, the Golgi apparatus, or vesicle secretion. Furthermore, comparison of data with our previous study examining protein rescue by MG132 or leupeptin indicated that GLG1, NEDD4 and CHST14 were also significantly rescued by treatment with the lysosomal protease inhibitor leupeptin (**Figure 3**), suggesting that a proportion of the proteins rescued by MG132 alone are degraded lysosomally.

Of proteins exhibiting a greater degree of rescue with bortezomib compared to MG132 (**Figure 2A, purple dots**), 8/9 (89%) exhibited MG132 rescue ratios >1.25 but <1.5 (examples in **Figure S2, 2C bottom panel**), suggesting that the majority of all proteins in this class were in fact rescued by both inhibitors. The one exception was LIM domain-containing protein AJUBA, whose MG132 rescue ratio was 1.16 in this data (**Figure 2C bottom panel**), but neared significance in our previous study (**Table S2**); these differences may reflect relatively poor quantitation by only two or one peptides respectively.
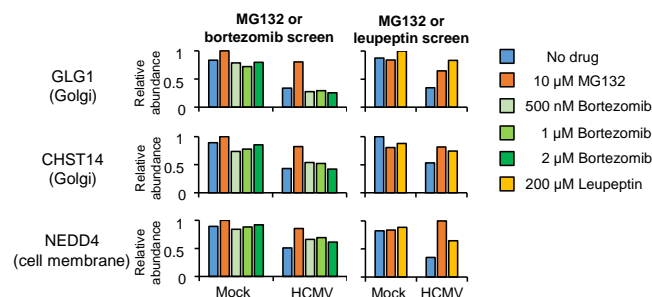
Figure 3

Figure 3. Proteins rescued by MG132 but not bortezomib are also rescued by Leupeptin.
Results for GLG1, NEDD4 and CHST14, proteins selectively rescued by MG132 but not bortezomib. The left hand panels show data from the complete MG132/bortezomib screen and the right hand panels show the MG132 (10 µM) /Leupeptin (200 µM) screen (12 hpi) described in Nightingale *et al* (Nightingale et al., 2018).

Discussion

HCMV is known to be a master regulator of host immunity, achieving lifelong persistence in infected individuals by utilising a wide range of strategies to modulate host protein expression. These include the deployment of proteins to target host factors for degradation. Here, we provide a searchable database that systematically details the route of degradation of cellular proteins during the establishment of a productive HCMV infection. Furthermore, this data can be used to predict molecules of key importance in antiviral

immunity to HCMV on the basis of their degradation.

MG132 is a less selective proteasomal inhibitor than bortezomib, having previously been reported to inhibit lysosomal degradation pathways via inhibition of calpains and cathespsins (Kisselev and Goldberg, 2001), in addition to the proteasome. In our previous publication, 75% of proteins rescued by leupeptin at 12h of infection were also rescued by MG132. The usefulness of comparing this broad proteasomal/lysosomal inhibitor with the specific proteasomal inhibitor bortezomib is the identification that 62-85% of proteins rescued by MG132 were also rescued by bortezomib, suggesting that the proteasome is the predominant route for early protein degradation during HCMV infection. Overall, of all *downregulated* proteins, 44% were rescued by at least one of MG132 or bortezomib. It is possible that in order to downregulate certain proteins, HCMV must employ degradative pathways in order to achieve sufficiently rapid change in protein abundance.

We and others have previously shown that membrane proteins are targeted for lysosomal degradation during HCMV infection (Weekes et al., 2013;Fielding et al., 2014;Hsu et al., 2015;Fielding et al., 2017), and data here identified that all proteins rescued by MG132 but not bortezomib had a membrane origin. Certain proteins were exclusively degraded by a non-proteasomal route, including GLG1 and CHST14. Extension of these inhibitor studies to examining membrane-enriched samples, for example samples enriched for plasma membrane proteins (Weekes et al., 2013;Weekes et al., 2014) would therefore be of substantial interest, and may identify a distinct degradative route for proteins originating from these compartments.

Comparison of data from this study with our previous transcriptional analysis of host gene expression during infection suggested that 54% of the 81 proteins with MG132 and bortezomib rescue ratios <1.5 were more than 1.5-fold transcriptionally downregulated, which would be expected to be a major mechanism of protein downregulation in the absence of degradation. The fold change cutoff of 1.5 for both downregulation by HCMV, and rescue by either inhibitor was based on a significance threshold of p<0.01, however had the effect of excluding proteins with 'borderline' rescue ratios of >1.25 but <1.5. 39/81 proteins with MG132 and bortezomib rescue ratios <1.5 exhibited rescue ratios for MG132 or bortezomib or both that were nevertheless >1.25, suggesting that this group of proteins included some candidates that downregulated by degradation, at least in part.

Overall, this analysis of host protein degradation during HCMV infection has not only identified proteasomal degradation as a key mechanism subverted by the virus early during infection, but has also generated a short-list of proteasomally degraded proteins enriched in known HCMV restriction factors. Further investigation into the role of the other proteins in this shortlist is warranted to determine if they also have restrictive capabilities. Identification of HCMV restriction factors, understanding the mechanism by which they restrict infection and identification of viral antagonists that target these factors for degradation are of fundamental interest due to the potential for therapeutic intervention.

Data Availability Statement

The datasets generated for this study will be deposited to the ProteomeXchange Consortium via the PRIDE partner repository.

Conflict of Interest

The authors declare that the research was conducted in the absence of any commercial or financial relationships that could be construed as a potential conflict of interest.

Author Contributions

K.-M.L., K.N. and M.P.W. designed the experiments. K.-M.L., K.N., and M.P.W. wrote the manuscript. K.-M.L., K.N., R.A., and M.P.W. performed the experiments. K.-M.L., K.N., L.S., and M.P.W. analysed the proteomics data. K.-M.L., K.N., L.S., and M.P.W. edited the manuscript. M.P.W. supervised all research.

Funding

References

Cannon, M.J., Schmid, D.S., and Hyde, T.B. (2010). Review of cytomegalovirus seroprevalence and demographic characteristics associated with infection. *Rev Med Virol* 20, 202-213.

Chen, D., Frezza, M., Schmitt, S., Kanwar, J., and Dou, Q.P. (2011). Bortezomib as the first proteasome inhibitor anticancer drug: current status and future perspectives. *Curr Cancer Drug Targets* 11, 239-253.

Chui, A.J., Okondo, M.C., Rao, S.D., Gai, K., Griswold, A.R., Johnson, D.C., Ball, D.P., Taabazuing, C.Y., Orth, E.L., Vittimberga, B.A., and Bachovchin, D.A. (2019). N-terminal degradation activates the NLRP1B inflammasome. *Science* 364, 82-85.

Cox, J., and Mann, M. (2008). MaxQuant enables high peptide identification rates, individualized p.p.b.-range mass accuracies and proteome-wide protein quantification. *Nat Biotechnol* 26, 1367-1372.

Dolan, A., Cunningham, C., Hector, R.D., Hassan-Walker, A.F., Lee, L., Addison, C., Dargan, D.J., Mcgeoch, D.J., Gatherer, D., Emery, V.C., Griffiths, P.D., Sinzger, C., Mcsharry, B.P., Wilkinson, G.W.G., and Davison, A.J. (2004). Genetic content of wild-type human cytomegalovirus. *J Gen Virol* 85, 1301-1312.

El Helou, G., and Razonable, R.R. (2019). Letermovir for the prevention of cytomegalovirus infection and disease in transplant recipients: an evidence-based review. *Infect Drug Resist* 12, 1481-1491.

Fielding, C.A., Aicheler, R., Stanton, R.J., Wang, E.C., Han, S., Seirafian, S., Davies, J., Mcsharry, B.P., Weekes, M.P., Antrobus, P.R., Prod'homme, V., Blanchet, F.P., Sugrue, D., Cuff, S., Roberts, D., Davison, A.J., Lehner, P.J., Wilkinson, G.W., and Tomasec, P. (2014). Two novel human cytomegalovirus NK cell evasion functions target MICA for lysosomal degradation. *PLoS Pathog* 10, e1004058.

Fielding, C.A., Weekes, M.P., Nobre, L.V., Ruckova, E., Wilkie, G.S., Paulo, J.A., Chang, C., Suárez, N.M., Davies, J.A., Antrobus, R., Stanton, R.J., Aicheler, R.J., Nichols, H., Vojtesek, B., Trowsdale, J., Davison, A.J., Gygi, S.P., Tomasec, P., Lehner, P.J., and Wilkinson, G.W. (2017). Control of immune ligands by members of a cytomegalovirus gene expansion suppresses natural killer cell activation. *Elife* 6.

Goodwin, C.M., Ciesla, J.H., and Munger, J. (2018). Who's Driving? Human Cytomegalovirus, Interferon, and NFκB Signaling. *Viruses* 10.

Griffiths, P., Baraniak, I., and Reeves, M. (2015). The pathogenesis of human cytomegalovirus. *J Pathol* 235, 288-297.

Halenius, A., Gerke, C., and Hengel, H. (2015). Classical and non-classical MHC I molecule manipulation by human cytomegalovirus: so many targets—but how many arrows in the quiver? *Cell Mol Immunol* 12, 139-153.

Hsu, J.L., Van Den Boomen, D.J., Tomasec, P., Weekes, M.P., Antrobus, R., Stanton, R.J., Ruckova, E., Sugrue, D., Wilkie, G.S., Davison, A.J., Wilkinson, G.W., and Lehner, P.J. (2015). Plasma membrane profiling defines an expanded class of cell surface proteins selectively targeted for degradation by HCMV US2 in cooperation with UL141. *PLoS Pathog* 11, e1004811.

Jackson, S.E., Mason, G.M., and Wills, M.R. (2011). Human cytomegalovirus immunity and immune evasion. *Virus Res* 157, 151-160.

Kim, Y.E., Lee, J.H., Kim, E.T., Shin, H.J., Gu, S.Y., Seol, H.S., Ling, P.D., Lee, C.H., and Ahn, J.H. (2011). Human cytomegalovirus infection causes degradation of Sp100 proteins that suppress viral gene expression. *J Virol* 85, 11928-11937.

Kisselev, A.F., and Goldberg, A.L. (2001). Proteasome inhibitors: from research tools to drug candidates. *Chem Biol* 8, 739-758.

Le-Trilling, V.T., and Trilling, M. (2015). Attack, parry and riposte: molecular fencing between the innate immune system and human herpesviruses. *Tissue Antigens* 86, 1-13.

Manicklal, S., Emery, V.C., Lazzarotto, T., Boppana, S.B., and Gupta, R.K. (2013). The "silent" global burden of congenital cytomegalovirus.*Clin Microbiol Rev* 26, 86-102.

Nathans, R., Cao, H., Sharova, N., Ali, A., Sharkey, M., Stranska, R., Stevenson, M., and Rana, T.M. (2008). Small-molecule inhibition of HIV-1 Vif. *Nat Biotechnol* 26, 1187-1192.

Nightingale, K., Lin, K.M., Ravenhill, B.J., Davies, C., Nobre, L., Fielding, C.A., Ruckova, E., Fletcher-Etherington, A., Soday, L., Nichols, H., Sugrue, D., Wang, E.C.Y., Moreno, P., Umrania, Y., Huttlin, E.L., Antrobus, R., Davison, A.J., Wilkinson, G.W.G., Stanton, R.J., Tomasec, P., and Weekes, M.P. (2018). High-Definition Analysis of Host Protein Stability during Human Cytomegalovirus Infection Reveals Antiviral Factors and Viral Evasion Mechanisms. *Cell Host Microbe*24, 447-460.e411.

Nobre, L.V., Nightingale, K., Ravenhill, B.J., Antrobus, R., Soday, L., Nichols, J., Davies, J.A., Seirafian, S., Wang, E.C., Davison, A.J., Wilkinson, G.W., Stanton, R.J., Huttlin, E.L., and Weekes, M.P. (2019). Human cytomegalovirus interactome analysis identifies degradation hubs, domain associations and viral protein functions. *Elife* 8.

Patel, M., Vlahava, V.M., Forbes, S.K., Fielding, C.A., Stanton, R.J., and Wang, E.C.Y. (2018). HCMV-Encoded NK Modulators: Lessons From in vitro and in vivo Genetic Variation. *Front Immunol* 9,2214.

Price, C.T., Al-Quadan, T., Santic, M., Rosenshine, I., and Abu Kwaik, Y. (2011). Host proteasomal degradation generates amino acids essential for intracellular bacterial growth. *Science* 334,1553-1557.

Reeves, M.B., Macary, P.A., Lehner, P.J., Sissons, J.G., and Sinclair, J.H. (2005). Latency, chromatin remodeling, and reactivation of human cytomegalovirus in the dendritic cells of healthy carriers. *Proc Natl Acad Sci U S A* 102, 4140-4145.

Schreiner, S., and Wodrich, H. (2013). Virion factors that target Daxx to overcome intrinsic immunity. *J Virol* 87, 10412-10422.

Sloan, E., Orr, A., and Everett, R.D. (2016). MORC3, a Component of PML Nuclear Bodies, Has a Role in Restricting Herpes Simplex Virus 1 and Human Cytomegalovirus. *J Virol* 90, 8621-8633.

Stanton, R.J., Baluchova, K., Dargan, D.J., Cunningham, C., Sheehy, O., Seirafian, S., Mcsharry, B.P., Neale, M.L., Davies, J.A., Tomasec, P., Davison, A.J., and Wilkinson, G.W. (2010). Reconstruction of the complete human cytomegalovirus genome in a BAC reveals RL13 to be a potent inhibitor of replication. *J Clin Invest* 120,3191-3208.

Tanaka, J., Ogura, T., Kamiya, S., Sato, H., Yoshie, T., Ogura, H., and Hatano, M. (1984). Enhanced replication of human cytomegalovirus in human fibroblasts treated with dexamethasone. *J Gen Virol* 65 (Pt 10), 1759-1767.

Tavalai, N., Adler, M., Scherer, M., Riedl, Y., and Stamminger, T. (2011). Evidence for a dual antiviral role of the major nuclear domain 10 component Sp100 during the immediate-early and late phases of the human cytomegalovirus replication cycle. *J Virol* 85,9447-9458.

Tran, K., Kamil, J.P., Coen, D.M., and Spector, D.H. (2010). Inactivation and disassembly of the anaphase-promoting complex during human cytomegalovirus infection is associated with degradation of the APC5 and APC4 subunits and does not require UL97-mediated phosphorylation of Cdh1. *J Virol* 84, 10832-10843.

Weekes, M.P., Tan, S.Y., Poole, E., Talbot, S., Antrobus, R., Smith, D.L., Montag, C., Gygi, S.P., Sinclair, J.H., and Lehner, P.J. (2013). Latency-associated degradation of the MRP1 drug transporter during latent human cytomegalovirus infection. *Science* 340**,**199-202.

Weekes, M.P., Tomasec, P., Huttlin, E.L., Fielding, C.A., Nusinow, D., Stanton, R.J., Wang, E.C.Y., Aicheler, R., Murrell, I., Wilkinson, G.W.G., Lehner, P.J., and Gygi, S.P. (2014). Quantitative temporal viromics: an approach to investigate host-pathogen interaction.*Cell* 157**,** 1460-1472.

Weirtz, E.J., Jones, T.R., Sun, L., Bogyo, M., Geuze, H.J., and Ploegh, H.L. (1996). The human cytomegalovirus US11 gene product dislocates MHC class I heavy chains from the endoplasmic reticulum to the cytosol.*Cell* 84**,** 769-779.

Supplementary Materials

Supplementary tables

Hosted file

Table_S1.xlsx available at https://authorea.com/users/332778/articles/464398-rapid-degradation-pathways-of-host-proteins-during-hcmv-infection-revealed-by-quantitative-proteomics

Table S1. Details of each group of proteins shown in Figure 2B. Each worksheet shows a different group of proteins illustrated in Figure 2B.

Hosted file

Table_S2.xlsx available at https://authorea.com/users/332778/articles/464398-rapid-degradation-pathways-of-host-proteins-during-hcmv-infection-revealed-by-quantitative-proteomics

Table S2. Interactive spreadsheet of all data in the manuscript. The "Plotter" worksheet enables generation of graphs for all of the proteins quantified, and easy visualization of statistics. The "Data" worksheet shows minimally annotated protein and transcript data, with only formatting and normalization modifying the raw data. The "Stats" worksheet shows the p-values for each fold change or rescue ratio.
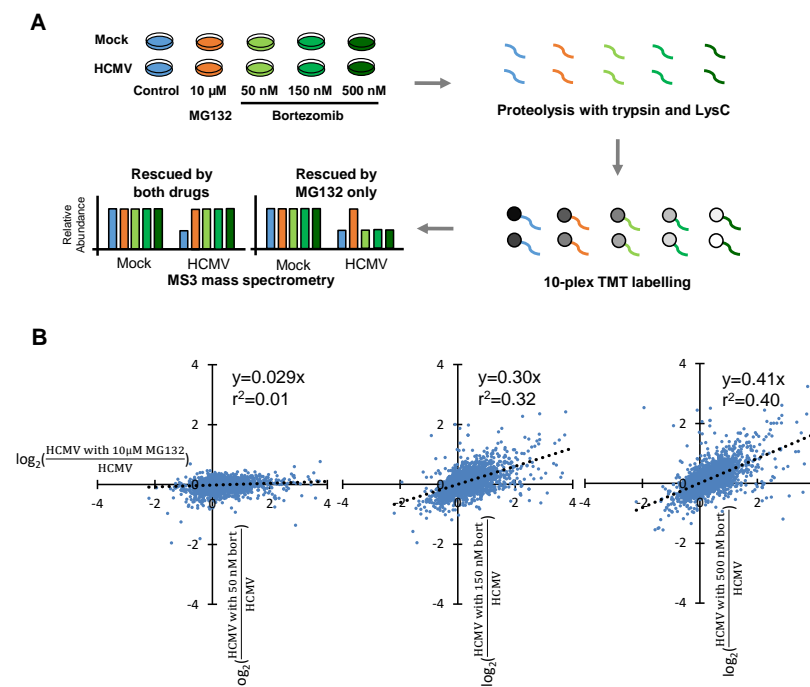
Hosted file

Table_S3.xlsx available at https://authorea.com/users/332778/articles/464398-rapid-degradation-pathways-of-host-proteins-during-hcmv-infection-revealed-by-quantitative-proteomics

Table S3. Details of TMT labelling used in this paper.

Supplementary figures

Figure S1

A

B

Φιγυρε Σ1. Οπτιμισατιον οφ βορτεζομιβ ςονςεντρατιον βψ ςομπαρισον ωιτη 10 μM ΜΓ132. (A) Schematic of the experimental workflow. HFFF-TERT cells were infected with Merlin strain HCMV (MOI 5) or mock infected. After 12h of infection, cells were treated with 10 μM MG132 or 50 nM, 150 nM or 500 nM of bortezomib for a further 12 h and harvested for analysis at 24 hpi. Whole cell lysates were digested into peptides, which were labelled with TMT reagents followed by MS3 mass spectrometry. (B) Comparison of 10 μM MG132 with 50 nM, 150 nM or 500 nM bortezomib (bort).
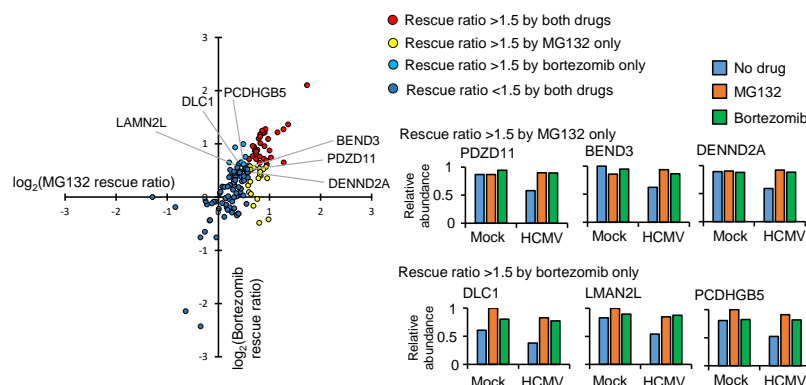
13

Figure S2

Figure S2. Examples of proteins exhibiting rescue ratios >1.5 with only one of two inhibitors, but a rescue ratio between 1.25 − 1.5 fold with the other inhibitor. Data is displayed as described in Figure 2.

Detailed materials and methods for proteomics analysis

Whole cell lysate protein digestion

Cells were washed with PBS once, typrsinised, neutralised with complete DMEM, pelleted, and lysed (6M Guanidine [Thermo]/50 mM HEPES [Sigma] pH 8.5). Lysates were sonicated for 2.5 min at constant 4°C cooling with Bioruptor Pico (Diagenode), and cell debris was removed by centrifugation at 21,000 xg for 10 min at 4°C. To reduce protein, dithiothreitol (DTT, Sigma) was added and samples were incubated for 20 min at room temperature. Cysteines were alkylated with 14 mM iodoacetamide (IAA, Sigma), incubated 20 min at room temperature in the dark, and excess IAA was quenched with DTT for 15 min. Guanidine

14

concentration was lowered to 1.5M with 200 mM HEPES (pH 8.5), then protein samples were digested with LysC protease (Wako) at a 1:100 protease-to-protein ratio for 3 h at room temperature. Guanidine concentration was further lowered to 0.5M and Trypsin (Thermo) was then added at a 1:100 protease-to-protein ratio followed by overnight incubation at 37 °C with constant shaking. Trypsin was quenched with 5% formic acid. Samples were then centrifuged at 21,000 xg for 10 min at 4°C to remove undigested protein. Peptides were subjected to octadecyl carbon chain (C18) solid-phase extraction (SPE, Sep-Pak, Waters) and dried with a speed-vac (Thermo).

Peptide Labelling with Tandem Mass Tags

Desalted peptides were dissolved in 200 mM HEPES (pH 8.5) and peptide concentration was measured by microBCA (Thermo). 2 µg of TMT reagents (dissolved in anhydrous acetonitrile [Acros organics]) was added to every µg of peptides at a final acetonitrile concentration of 30% (v/v) and incubated at room temperature for 1 h. The TMT-10plex isobaric label reagent set (Thermo) was used for labelling. Sample labelling was as indicated in Table S3. The reaction was quenched with 0.3% (v/v) hydroxylamine (Thistle Scientific). Equal amounts of TMT-labelled samples were combined and subjected to C18 SPE then dried by speed-vac before being subjected to high pH reversed phase fractionation (HpRP) or mass spectrometry.

Offline High pH Reversed-Phase Fractionation

TMT-labelled peptides were fractionated using an Ultimate 3000 rapid separation (RS) nano UHPLC system (Thermo), generating 12 combined fractions. The system is equipped with a Kinetex Evo C18 column (Phenomenex) that has 2.1 mm in internal diameter (ID) and is 25 cm in length, filled with C18 bound silica particles with diameter of 1.7 µm. Mobile phase was HPLC grade H_2O, acetonitrile, and ammonium formate (pH 10). The concentration of ammonium formate was maintained at 20 mM while concentration of acetonitrile gradually increased throughout the fractionation elution programme. Starting from 2.7% (v/v), acetonitrile concentration increased to 21% in the first 10 min, to 36% after 24 min 15 sec of elution, then to 51% after 33 min of elution. Acetonitrile concentration was subsequently increased and maintained at 90% for 10 min to wash the column. The flow rate was 400 ml/min and the elution was performed at 45°C. UV absorbance was monitored at 280 nm and fractions were collected into 96 well microplates using the integrated fraction collector. Fractions were recombined orthogonally in a checkerboard fashion, combining alternate wells from each column of the plate into a single fraction, and commencing combination of adjacent fractions in alternating rows. Wells were excluded prior to the start or after the cessation of elution of peptide-rich fractions, as identified from the UV trace. This resulted into two sets of 12 combined fractions, which were dried in a vacuum centrifuge and resuspended in 10 ml solvent (4% acetonitrile and 5% formic acid) prior to LC-MS3.

Liquid chromatography coupled with multi-stage mass spectrometry (LC-MS3)

An Ultimate 3000 RSLC nano UHPLC was used for online fractionation, equipped with a 300 µm ID x 5 mm Acclaim PepMap µ-Precolumn (Thermo) and a 75 µm ID x 50 cm 2.1 µm particle Acclaim PepMap RSLC analytical column (Thermo). Loading solvent was 0.1% formic acid. Analytical solvent contained HPLC grade H_2O, acetonitrile, and formic acid. Samples were loaded at 5 ml/min for 5 min in loading solvent before beginning the analytical gradient. Formic acid concentration was maintained at 0.1% during the analytical gradient while concentration of acetonitrile gradually increased. All separations were carried out at 55 °C. Mass spectrometry data were acquired using Orbitrap Lumos mass spectrometer (Thermo). TMT-based analysis used a MultiNotch MS3-based method (McAlister et al., 2014). MS1 scans surveyed 380-1500 Th, with resolution of 120,000, automatic gain control (AGC) target of 2×10^5, and maximum injection time of 50 ms. Ions that had the counts of 5×10^3 counts and above triggered MS2 analysis, with Quadrupole isolation at an isolation width of 0.7 Th, normalised collision energy (NCE) set to 35% for CID fragmentation, 1.5×10^4 AGC target, and 120 ms maximum injection time. Top 6 MS2 ions were selected for HCD fragmentation (NCE 65%) in MS3. MS3 resolution was 60,000, with an AGC target of 1×10^5 and a maximum accumulation time of 150 ms. The entire MS/MS/MS cycle had a target time of 3 sec. Dynamic exclusion was set to +/- 10 ppm for 70 sec.

15

Protein Quantification

Mass spectra were processed using "MassPike", which is a SEQUEST-based software for quantitative proteomics, developed by Professor Steven Gygi and colleagues at Harvard Medical School. In MassPike, MS spectra were converted to mzXML format using an extractor built upon Thermo Fisher's RAW File Reader library (version 4.0.26). The standard mzXML format has been augmented during extraction and conversion, with additional customisations that are specific to ion trap and Orbitrap mass spectrometry and essential for TMT quantitation. These customisations consider ion injection times for each scan, Fourier Transform-derived baseline and noise values calculated for every Orbitrap scan, isolation widths for each scan type, scan event numbers, and elapsed scan times.

Mass spectra acquired were searched against a combined protein sequence database that includes human proteins, HCMV proteins, and possible protein contaminants that might be introduced to samples. The human protein Uniprot database was downloaded on 26[th]January, 2017. An HCMV protein database was assembled from the HCMV strain Merlin Uniprot database, non-canonical human cytomegalovirus ORFs described by Stern-Ginossar et al (23180859), and a six-frame translation of HCMV strain Merlin filtered to include all potential ORFs of [?]8 residues (delimited by stop-stop rather than requiring ATG-stop). The database also included common contaminants (bovine serum albumin and porcine trypsin, and annotated human protein contaminants such as keratins). Searches were performed using a 20 ppm precursor ion tolerance. Fragment ion tolerance was set to 1.0 Th.

TMT tags on lysine residues and peptide N termini (229.162932 Da) and carbamidomethylation of cysteine residues (57.02146 Da) were set as static modifications, while oxidation of methionine residues (15.99492 Da) was set as a variable modification.

Peptide identification was executed in the order of the ranks using cross-correlation score (XCorr), as the correctness of peptide spectral matches (PSMs) decreased along the ranks. A target-decoy strategy was employed to ensure the quality of peptide identification (Elias and Gygi, 2007). A decoy database was generated by reversing the sequence of the composite protein database detailed above. Assignment of peptides from this decoy database were considered as a "false discovery", and peptide identification terminated before the false discovery rate reached 1%. Correct and incorrect spectral matches were distinguished from one another using linear discriminant analysis based on several different parameters including XCorr, the XCorr difference between top and second possible peptide (ΔCn), precursor mass error, and charge state.

Protein assembly was performed by principles of parsimony to produce the smallest set of proteins necessary to account for all observed peptides, meaning in cases of redundancy, shared peptides were assigned to the protein sequence with the greatest number of matching unique peptides.

Following fragmentation, each TMT tag produces reporter ions with specific mass, which were surveyed in low m/z area of the MS3 spectrum. The maximum intensity nearest to the theoretical m/z of each reporter ion was used. Proteins were quantified by summing TMT reporter ion counts across all matching peptide-spectral matches. If a TMT experiment uses n (number) types of TMT tags, more than n-1 TMT channels missing and/or a combined signal-to noise ratio of less than 25n across all TMT reporter ions were considered poor quality of MS3 spectra. PSMs with poor or no MS3 spectra were excluded from quantitation. Protein quantitation values were exported for further analysis in Excel. The method of significance A was used to estimate the p-value that each ratio was significantly different to 1 using Perseus version 1.5.1.6. Values were adjusted for multiple hypothesis testing using the method of Benjamini-Hochberg (Cox and Mann, 2008).

References related to detailed materials and methods for proteomics analysis

Cox, J., and Mann, M. (2008). MaxQuant enables high peptide identification rates, individualized p.p.b.-range mass accuracies and proteome-wide protein quantification. *Nat Biotechnol* 26**,**1367-1372.

Elias, J.E., and Gygi, S.P. (2007). Target-decoy search strategy for increased confidence in large-scale protein identifications by mass spectrometry. *Nat Methods* 4**,** 207-214.

Mcalister, G.C., Nusinow, D.P., Jedrychowski, M.P., Wühr, M., Huttlin, E.L., Erickson, B.K., Rad, R., Haas, W., and Gygi, S.P. (2014). MultiNotch MS3 enables accurate, sensitive, and multiplexed detection of differential expression across cancer cell line proteomes. *Anal Chem* 86**,** 7150-7158.